



This is the accepted manuscript made available via CHORUS, the article has been published as:

Numerical Modeling of the Sensitivity of X-Ray Driven Implosions to Low-Mode Flux Asymmetries

R. H. H. Scott, D. S. Clark, D. K. Bradley, D. A. Callahan, M. J. Edwards, S. W. Haan, O. S. Jones, B. K. Spears, M. M. Marinak, R. P. J. Town, P. A. Norreys, and L. J. Suter

Phys. Rev. Lett. **110**, 075001 — Published 14 February 2013

DOI: [10.1103/PhysRevLett.110.075001](https://doi.org/10.1103/PhysRevLett.110.075001)

Numerical Modeling of the Sensitivity of X-Ray Driven Implosions to Low-Mode Flux Asymmetries

R.H.H. Scott,^{1,*} D.S. Clark,² D.K. Bradley,² D.A. Callahan,² M.J. Edwards,² S.W. Haan,² O.S. Jones,² B.K. Spears,² M.M. Marinak,² R.P.J. Town,² P.A. Norreys,^{1,3} and L.J. Suter²

¹*Central Laser Facility, STFC Rutherford Appleton Laboratory,
Harwell Oxford, Didcot, OX11 0QX, United Kingdom*

²*Lawrence Livermore National Laboratory, Livermore, CA 94551, United States of America*

³*Department of Physics, University of Oxford, Parks Road, Oxford OX1 3PU, United Kingdom*

The sensitivity of inertial confinement fusion implosions, of the type performed on the National Ignition Facility (NIF) [1], to low-mode flux asymmetries has been investigated numerically. It is shown that large-amplitude, low-order mode shapes (Legendre polynomial P_4), resulting from low order flux asymmetries, cause spatial variations in capsule and fuel momentum that prevent the DT “ice” layer from being decelerated uniformly by the hot spot pressure. This reduces the transfer of implosion kinetic energy to internal energy of the central hot spot, thus reducing neutron yield. Furthermore, synthetic gated x-ray images of the hot spot self-emission indicate that P_4 shapes may be unquantifiable for DT layered capsules. Instead the positive P_4 asymmetry “aliases” itself as an oblate P_2 in the x-ray images. Correction of this apparent P_2 distortion can further distort the implosion while creating a round x-ray image. Long wavelength asymmetries may be playing a significant role in the observed yield reduction of NIF DT implosions relative to detailed post-shot 2D simulations.

Indirect-drive inertial confinement fusion (ICF) [1–3] uses lasers to heat the inside of a high-Z cavity (or hohlraum). The absorbed laser energy is re-emitted as x-rays. These x-rays heat the outer surface of a hollow, spherical, low-Z shell that contains a layer of frozen Deuterium and Tritium (DT) fuel. The heated outer shell ablates, creating a rocket-like reaction force, spherically imploding the shell at extremely high velocity (~ 350 km/s). During the implosion, spherical convergence causes the pressure in the central gaseous void (or hot spot) within the shell to rise. This pressure decelerates the shell, both compressing the solid fuel, and converting the shell’s kinetic energy into hot spot internal energy, thus heating the hot spot, thereby initiating DT fusion reactions. Provided the hot spot areal density is sufficient, α -particles will further heat the hot spot, causing bootstrap heating, ignition and thermonuclear burn propagation into the surrounding cold fuel. Numerical modeling indicates that the NIF can, for the first time, initiate inertial fusion ignition in the laboratory [4–6]. In comparison to detailed post-shot simulations [7], current NIF DT layered capsule implosions have neutron yields reduced by $\sim 3 - 10\times$ and hotspot masses reduced by $2 - 3\times$ [8, 9], while hot spot temperatures are similar. Low mode capsule shape distortions may explain some of this apparent discordancy [10], as simulations indicate they can reduce the conversion of implosion kinetic energy to hotspot internal energy, thereby bringing hot spot mass, energy, temperature and neutron yield more in line with experiments.

In this Letter, the effects of low-mode capsule shape asymmetries are examined numerically. The non-uniformity of the x-ray flux incident upon the shell and the resultant shell shapes can be described mathemati-

cally as a series of Legendre polynomials [11]. It is shown that a P_4 implosion asymmetry, that might result from low-order hohlraum generated flux asymmetries, causes spatial variations in the capsule & fuel momentum. This inhibits uniform deceleration of the capsule and fuel by the hot spot pressure, reducing the transfer of implosion kinetic energy to hot spot internal energy thus significantly reducing the capsule performance. Furthermore, simulated gated x-ray images of the hot spot self-emission show reduced sensitivity to the P_4 mode, instead the images appear to have a pronounced oblate P_2 shape. Reducing the amplitude of the oblate P_2 shape (as measured from the x-ray image) further reduces the sensitivity to the P_4 mode meaning the resulting x-ray images are round despite the capsule shape being highly distorted. Comparisons are made between key physical properties of the implosion, synthetically generated experimental observables, and NIF data.

The indirect-drive approach to ICF smooths high mode spatial non-uniformities in the x-ray flux incident upon the capsule, however the spatial distribution of the cones of laser beams which illuminate the hohlraum means that low mode x-ray flux non-uniformities can occur [1], these are considerably lower mode than those recently examined by Thomas *et al* [12]. Capsule-only, two-dimensional (2D), cylindrically-symmetric geometry simulations were performed with the radiation-magnetohydrodynamics code Hydra [13]. These were driven by an x-ray drive taken from an integrated hohlraum simulation which was adjusted to match the shock timing data from the VISAR diagnostic [14, 15] from NIF shot N110521, and the capsule implosion trajectory [16] measured on NIF shot N110625. QEOS [17] was used with tabular opacities and multi-group radia-

tion diffusion. The effects of hohlraum P_4 flux asymmetries were investigated by perturbing the applied flux with a P_4 distribution function of amplitude varying from +10% to -10%. 2D Hydra modeling of the hohlraum & capsule [18] suggests the P_4 flux asymmetry incident on the capsule would be expected to be < 3%, except for in the first ~ 2 ns of the laser pulse where the flux asymmetry can be up to 10%. To date there is no direct measure of NIF hohlraum radiation asymmetry. The flux asymmetries were applied during the discrete time intervals 0 – 2 ns (the ‘picket’ [19]), 2 – 11.5 ns (the ‘trough’), 11.5 – 14 ns (2^{nd} shock), 14 – 16 ns (3^{rd} shock) and 16 – 18 ns (4^{th} rise) and 18 – 21.5 ns (peak drive), creating > 200 2D modeling runs of both DT layered capsules and DHe³ gas filled capsules with a surrogate CH ‘fuel’ mass (symmetry capsules). In order to recreate images from the NIF gated x-ray diagnostic [20](GXD), time resolved, 11 μm resolution, synthetic gated x-ray images of the hot spot self-emission > 6 keV, were created from polar and equatorial directions by post processing the Hydra runs. Hot spot and synthetic GXD shapes were characterised by a Legendre polynomial decomposition of the appropriate contour. The hot spot contour is defined as the minimum radius where $T_{e_j} > \frac{1}{2}T_{e_{j_{max}}}$ and $\rho_j < \frac{1}{2}\rho_{j_{max}}$ where T_e is the electron temperature and ρ the mass density, ‘max’ denotes the maximum value within the j^{th} angular ‘strip’ of cells. This is a robust definition of the hot spot even for highly distorted implosions. Based on previous studies the 17% contour of the GXD is used both for the synthetic GXD and experimentally.

The applied Legendre P_4 flux asymmetries induce P_4 hot spot shapes at stagnation (see Figs. 1 (a) & (c)), the sign of which is dependent on the timing of the applied flux asymmetry. If the asymmetry is present only during the shock compression phase (the first ~ 18 ns), shocks created in regions of the capsule exposed to higher flux propagate faster, these break out of the inner DT ice layer earlier, causing these regions to move ahead. This also causes ablator mass to flow laterally, away from the high flux region. Consequently during peak drive the regions initially exposed to high flux are at smaller radii, meaning they are accelerated less efficiently by the hohlraum flux and gain less total momentum. They can also have less aerial density (ρr). The net effect is that the regions experiencing high flux during shock compression will protrude outwards at stagnation. Conversely if the flux asymmetry is applied during peak drive, the regions of the capsule exposed to more flux gain more momentum, and protrude inwards at stagnation. Regardless of the timing of the applied asymmetry, during the stagnation phase of the implosion, pressure within the lower density hot spot decelerates the higher density fuel from peak velocity, making any perturbation on this interface grow due to the Rayleigh-Taylor instability [21, 22], in addition to the Bell-Plesset growth due to convergence

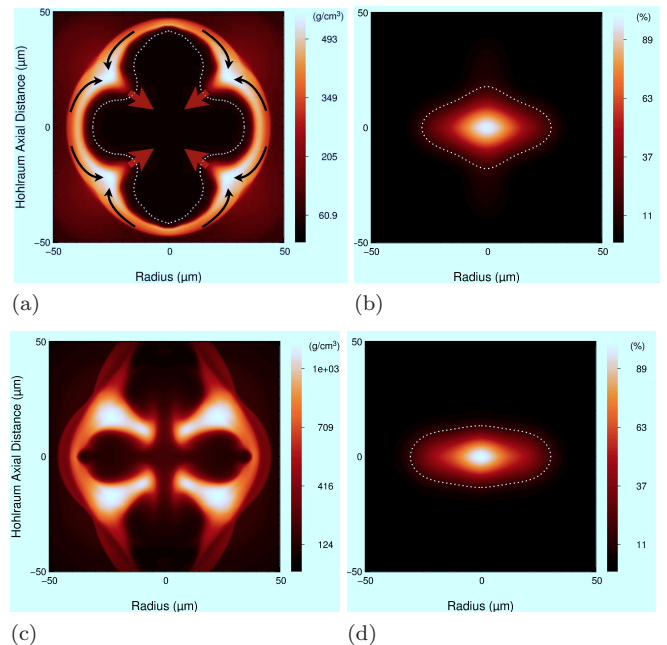


Figure 1. Axis of rotational symmetry is vertical at Radius = 0 μm . (a) DT layered capsule density plot at x-ray bangtime showing a positive Legendre polynomial P_4 shape. This simulation had a 10% flux asymmetry applied from 11.5-14 ns. Black arrows indicate the mass flows which occur during stagnation. After bangtime ‘fingers’ of fuel continue to flow inwards (red arrows). White dots depict the hot spot contour. (b) Synthetic gated x-ray image of the hot spot self-emission from 1(a), white dots show the 17% contour, a_4 is greatly reduced compared to fig. 1(a). (c) The same implosion as fig. 1(a), but 100 ps later. Large a_4 brings the bangtime earlier, meaning this image is plotted at the neutron bangtime of an equivalent spherical implosion. (d) The synthetic GXD from 1(c), showing a large negative (oblate) P_2 and almost zero a_4 despite the obvious P_4 in 1(c).

[23]. As the perturbations become larger, velocity shear between the hot spot and cold fuel perturbations can lead to the Kelvin-Helmholtz instability [24, 25], as visible at the tips of the inward protruding ‘fingers’ in fig. 1(c).

Figure 2 summarizes the scalings of some important DT layered capsule implosion parameters as a function of hot spot a_4 , all values are extracted from the simulations at x-ray bangtime. Fig. 2(a) depicts the ‘burn averaged’ ρr (the burn average of a quantity $Q_b = (\sum_{t=0}^{t=\infty} Q_t E_{prod} dt) / \int_{t=0}^{t=\infty} E_{prod} dt$ where Q_t is Q at time t and E_{prod} the thermonuclear energy production rate in time dt) as a function of hot spot a_4 . Although the spatially averaged ρr is relatively constant, the lateral mass flows caused by the P_4 can create large spatial variations in ρr . The regions with higher momentum continue to propagate radially inwards; fig. 2(b) depicts the remaining capsule kinetic energy (integrated from the hot spot surface to the ablation front) as a function of a_4 , and the partition of that energy into hot spot internal

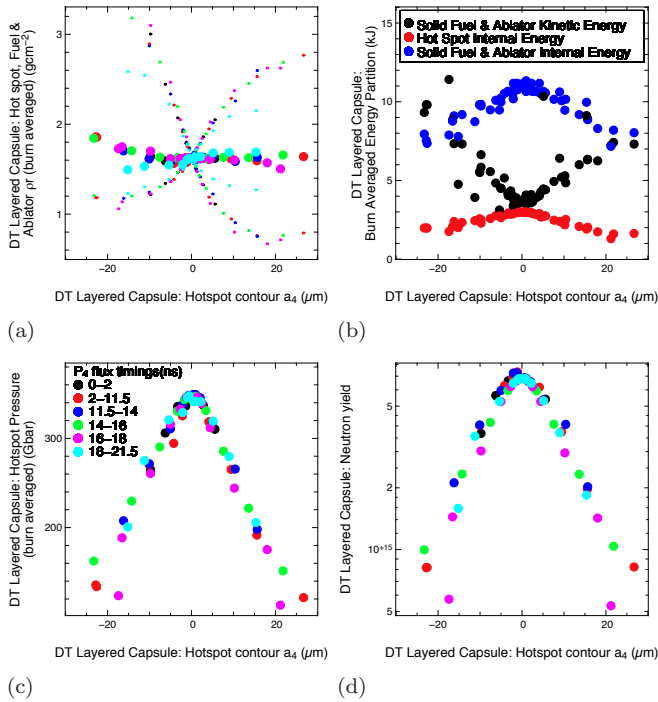


Figure 2. In (a), (c) and (d), colors depict timing of applied flux asymmetry, see (c) for legend. (a) Burn averaged hot spot + fuel + ablator ρr vs hot spot a_4 at x-ray bangtime: large dots depict spatially averaged ρr , while the smaller points are the corresponding maxima and minima in ρr . Large spatial variations in ρr occur due to P_4 . (b) The burn averaged energy partition as a function of hot spot a_4 ; increasing P_4 perturbations prevent the kinetic energy of the solid fuel + remaining ablator (black) from being converted to both hot spot internal energy (red) and solid fuel + remaining ablator internal energy (blue) during stagnation. (c) Burn averaged hot spot pressure as a function of hot spot a_4 . (d) Total thermonuclear neutron yield as a function of hot spot a_4 ; yield varies by a factor of 15 over the asymmetry range examined.

energy (integrated outwards to the hot spot surface) and solid fuel + ablator internal energy (integrated from the hot spot surface to the ablation front). For large a_4 less of the implosion kinetic energy is converted into hot spot internal energy and the hot spot pressure is reduced (fig. 2(c)). The reduction in neutron yield can be as large as $15\times$ for hot spot $a_4 = 20 \mu\text{m}$ (flux asymmetry $\sim 10\%$) as shown in fig. 2(d)).

Analysis of the synthetic GXD images suggests that the a_4 measured experimentally with the GXD is not a true representation of the hot spot a_4 , particularly for large positive a_4 . Fig. 3(a) depicts the relationship between the DT layered capsule hot spot a_4 and that of the synthetic GXD at x-ray bangtime (using the previously defined contours). The a_4 measured from the synthetic GXD is consistently lower than that of the hot spot. The insensitivity to positive hot spot a_4 is caused by lateral ablator mass flows which accumulate at $\sim 45^\circ$ (see Fig. 1 (a)) and reduce at the equator and poles. The abla-

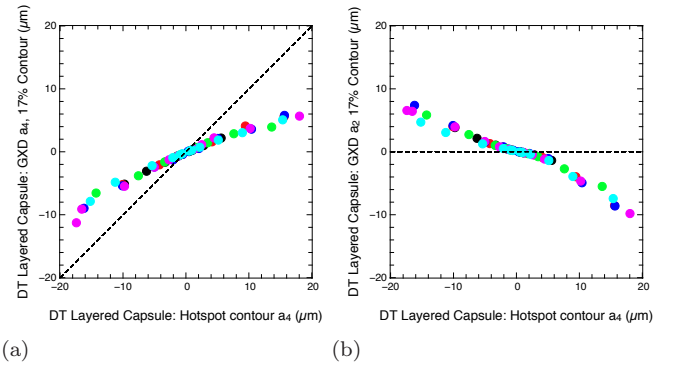


Figure 3. (a) Synthetic GXD a_4 plotted against DT layered capsule hot spot a_4 ; particularly for large positive a_4 the GXD is unable to effectively measure the amplitude of the P_4 mode. (b) Synthetic GXD a_2 plotted against DT layered capsule hot spot a_4 ; for large a_4 the GXD measures a significant P_2 mode amplitude despite the DT layered capsule hot spot $a_2 = 0 \pm 1 \mu\text{m}$ (not shown).

tor material is rotationally symmetric about the vertical axis, so the accumulated material absorbs the x-rays emitted from the polar-lobes of the hot spot (top and bottom), while allowing x-rays to more readily pass through the equatorial regions (left and right). Consequently the polar-lobes of the hot spot are almost completely invisible in the synthetic GXD plots. This causes the x-ray image to have a negative (oblate) P_2 shape. As the hot spot $a_2 = 0 \pm 1 \mu\text{m}$ (a_2 is the amplitude of the P_2 mode) for all these pure P_4 modelling runs, the P_2 inferred from the x-ray image is a “false” negative P_2 mode. This suggests that a negative P_2 mode measured from the self-emission x-ray image may in fact be a signature of a positive P_4 mode, although it does not preclude the presence of a true P_2 mode. Fig. 3(b) quantifies this aliasing effect. Symmetry capsules are qualitatively and quantitatively very similar. This is potentially important for the interpretation of GXD images from NIF DT implosions, which often exhibit negative P_2 modes [26].

In comparison to detailed 2D post-shot Hydra simulations [7], DT implosions on the NIF currently have yields reduced by $\sim 3 - 10\times$, while hot spot temperatures are similar. The inferred [8, 9] experimental hot spot volumes are increased in comparison to the post-shot simulations, while the hot spot mass is reduced, causing a $2 - 3\times$ reduction in the hotspot density. P_4 shape perturbations provide a mechanism which may explain these experimental observations, in particular bringing the yield and ion temperature relationship into better agreement. In the simulations discussed in this Letter, the DT fuel and hot spot do not mix; clear boundaries still exist (note these simulations use smooth capsules, but when nominal realistic capsule surface roughness [27] was employed and modes up to 200 resolved, no significant implosion degradation occurred for the full range of a_4). Consequently,

Implosion Parameter	NIF expt. range[8]	Hydra ($a_4 = 0 \mu\text{m}$)	Hydra ($a_4 = 20 \mu\text{m}$)
Hot spot internal energy (kJ)	0.7-1.4	3.1	1.3
Hot spot mass (μg)	2-6.4	8	5.5
X-ray P_0 (μm)	25-30	18.0	23.3
X-ray M_0 (μm)	25-35	17.0	27.1
Ion Temperature (keV)	3.3-4.4	3.9	3.9
Fuel ρr (gcm^{-2})	0.77-0.98	0.7	0.72
Yield (neutrons $\times 10^{14}$)	1.9-6.0	74	5.3

Table I. A comparison of NIF DT layered capsule experimental data from 4 shots N110608-N110908 with two Hydra implosions, one spherical ($a_4 = 0 \mu\text{m}$), and another with $a_4 = +20 \mu\text{m}$. Large positive P_4 brings the modeled implosion observables approximately in line with the experimental data. P_0 and M_0 are the amplitude of the 0th Legendre polynomial from the 17% contour of the equatorial and polar x-ray images respectively.

unlike high mode ‘mix’ [1] (where the hot spot can be radiatively cooled by high Z impurities), the simulated ion temperature inferred from the neutron spectrum remains unaffected at 3.9 ± 0.05 keV for all a_4 . The large a_4 does however truncate the thermonuclear burn, moving both the neutron and x-ray bangtimes earlier in time, so the capsule is still converging at bangtime. This, combined with the reduction in conversion of kinetic energy into internal energy, means the hot spot volume is increased. The hot spot mass decreases with positive a_4 , bringing Hydra simulations approximately in line with experimental data, as shown in Table I. This compares NIF experimental data with two Hydra implosions; one is perfectly spherical while the other has a hot spot a_4 of $+20 \mu\text{m}$ (flux asymmetry 10%). Notable features of implosions with large positive a_4 , all of which bring the simulations towards the data, are, the significantly reduced yield, reduced hot spot internal energy, reduced hot spot mass, unchanged ion temperature, increased x-ray image sizes, and hence increased hot spot volume, which reduces pressure and density, and finally, large spatial variations in ρr . We must emphasize, however, that this should not be interpreted as conclusive evidence that a P_4 asymmetry is responsible for the observed reduced NIF capsule performance. Although this study has concentrated on the P_4 mode, it is likely that all low modes would reduce the conversion of capsule kinetic energy into hot spot internal energy, and may result in similar ambiguity in the shape of the x-ray emission from the hot spot [28].

As discussed, implosions with a significant P_4 asymmetry can have a very apparent but ‘false’ P_2 asymmetry in GXD images. We find that attempting to correct this ‘false’ P_2 by increasing laser power to the hohlraum waist (the capsule equator) [26] can lead to a round GXD image even though the correction actually produces a more distorted DT fuel ice layer. This is depicted in fig. 4 for the case of a DT layered capsule where we applied

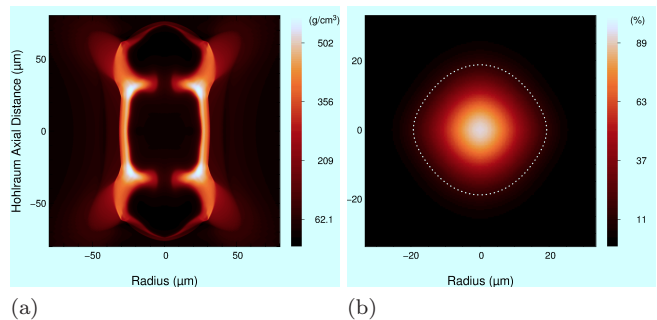


Figure 4. (a) Density plot of a DT layered capsule run with both P_2 and P_4 flux modes applied. Axis of rotational symmetry is vertical at Radius = $0 \mu\text{m}$. (b) The equatorial synthetic GXD image of fig. 4(a) at the same time, dotted line shows 17% contour. Despite the highly non-spherical density distribution in fig. 4(a), the equatorial GXD image is almost perfectly round. Note the spatial scales of (a) and (b) differ for clarity.

and empirically adjusted a P_2 flux asymmetry, in addition to the original P_4 , in order to make the synthetic GXD image appear round. As the applied P_2 flux is increased in order to reduce the ‘false’ GXD a_2 towards zero, there is a marked additional reduction in sensitivity to the a_4 measured from the x-ray image relative to that shown in Fig. 3(a) - in this simulation hot spot $a_4 = 25 \mu\text{m}$ and GXD $a_4 = 1 \mu\text{m}$. This suggests that attempts to tune the hohlraum to eliminate a ‘false’ P_2 can have the unintended consequence of exacerbating overall asymmetry, while further reducing the diagnostic sensitivity to the asymmetry. A corollary of figure 4, is that it is possible to create imploded configurations which appear to be spherical based on both orthogonal GXD images but, in fact, are significantly asymmetric and have greatly reduced performance in comparison to equivalent spherical implosions because a large fraction of the imploding shell’s kinetic energy remains unstagnated.

The Science of Fusion Ignition Workshop [30] identified the understanding of the origin of the measured ρr asymmetries as a high priority. Experiments are currently being developed on the NIF to measure low mode asymmetry of the ablator in-flight using x-ray backlighting [16], and of the DT fuel at stagnation using Compton radiography [29]. These will eliminate the degeneracy in inferring implosion asymmetry from hot spot x-ray emission, as identified in this Letter. The P_4 x-ray drive asymmetry may be modified by re-pointing the laser beams within the hohlraum, moving the laser hot spots relative to the capsule. Large beam re-pointing may require changing the hohlraum length in order for the laser beams to pass cleanly through the laser entrance holes.

In summary, numerical simulations have been used to examine the sensitivity of implosions similar to those currently taking place on NIF to low-mode flux asymmetries. It is shown that Legendre polynomial P_4 flux

modes induce P_4 shape modes at the time of capsule stagnation. The largest P_4 amplitudes studied in this Letter can cause up to 50% of the capsule kinetic energy to remain unconverted to hot spot and DT ice internal energy, in turn reducing the neutron yield by up to $15\times$. Simulated x-ray images of the hot spot self-emission show reduced sensitivity to the positive P_4 mode, instead the images appear to have a pronounced oblate P_2 shape. Attempting to correct for this apparent P_2 distortion can further distort the implosion while creating x-ray images which appear round and self-consistent from both equatorial and polar directions. This also further reduces the sensitivity to the P_4 mode such that that no quantitative evaluation of the hot spot a_4 can be made. Long wavelength asymmetries may be playing a significant role in the observed yield reduction of NIF DT implosions relative to detailed post-shot 2D simulations.



* Robbie.Scott@stfc.ac.uk; Also visiting scientist at Lawrence Livermore National Laboratory, Livermore, CA 94551, United States of America, & Department of Physics, The Blackett Laboratory, Imperial College London, Prince Consort Road, London, SW7 2AZ, United Kingdom. The authors thank M.H. Key, O.L. Landen and C. Cerjan for useful discussions, the staff of NIF and Livermore Computing. RHHS and PAN were supported by the UK Science and Technology Facilities Council. The work was performed for the U.S. Department of Energy by LLNL under Contract DE-AC52-07NA27344.

- [1] J. D. Lindl *et al.*, Physics of Plasmas **11**, 339 (2004).
- [2] N. Basov, Edward teller lectures (1991).
- [3] J. NUCKOLLS *et al.*, Nature **239**, 139 (1972).
- [4] S. W. Haan *et al.*, Physics of Plasmas **18**, 051001 (2011).
- [5] D. S. Clark *et al.*, Phys. Plasmas **17**, 052703 (2010).
- [6] D. A. Callahan *et al.*, Journal of Physics: Conference Series **112**, 022021 (2008).
- [7] D. Clark *et al.*, Physics of Plasmas (*Submitted*) (2012).
- [8] P. T. Springer and C. Cerjan, in *IFSA Proceedings Bordeaux, France* (2011).
- [9] C. Cerjan, P. T. Springer and S. M. Sepke, Physics of Plasmas, Submitted.
- [10] B. K. Spears *et al.*, Physics of Plasmas **19**, 056316 (2012).
- [11] M. Abramowitz and I. A. Stegun, *Handbook of Mathematical Functions with Formulas, Graphs, and Mathematical Tables*, volume pp. 331-339 and 771-802, Dover (1972).
- [12] V. A. Thomas and R. J. Kares, Phys. Rev. Lett. **109**, 075004 (2012).
- [13] M. M. Marinak *et al.*, Physics of Plasmas **8**, 2275 (2001).
- [14] L. M. Barker and R. E. Hollenbach, Journal of Applied Physics **43**, 4669 (1972).
- [15] H. F. Robey *et al.*, Physics of Plasmas **19**, 042706 (2012).
- [16] D. G. Hicks *et al.*, Physics of Plasmas **19**, 122702 (2012).
- [17] R. M. More *et al.*, Physics of Fluids **31**, 3059 (1988).
- [18] O. S. Jones, Private Communication, (2012).
- [19] H. F. Robey *et al.*, Phys. Rev. Lett. **108**, 215004 (2012).
- [20] J. A. Oertel *et al.*, Rev. of Sci. Instrum. **77**, 10E308 (2006).
- [21] L. Rayleigh, *Scientific Papers*, Cambridge University Press, Cambridge, England (1900).
- [22] G. I. Taylor, *The Instability of Liquid Surfaces when Accelerated in a Direction Perpendicular to their Planes. I*, Proc. R. Soc. London, Ser. A (1950).
- [23] R. Epstein, Physics of Plasmas **11**, 5114 (2004).
- [24] W. Kelvin, *Hydrokinetic solutions and observations*, London, Edinburgh Dublin Philos. Mag. J. Sci. 42, 362 (1871).
- [25] H. Helmholtz, *On discontinuous movements of fluids*, London, Edinburgh Dublin Philos. Mag. J. Sci. 36, 337 (1868).
- [26] S. H. Glenzer *et al.*, Science **327**, 1228 (2010).
- [27] D. S. Clark *et al.*, Physics of Plasmas **18**, 082701 (2011).
- [28] B.K. Spears, Private Communication, (2012).
- [29] R. Tommasini *et al.*, Physics of Plasmas **18**, 056309 (2011).
- [30] *Science of Fusion Ignition On NIF*, LLNL internal report, LLNL-TR-570412.